



Published in final edited form as:

Nature. 2005 August 11; 436(7052): 807–811. doi:10.1038/nature03845.

Evasion of the p53 tumour surveillance network by tumour-derived *MYC* mutants

Michael T. Hemann^{1,*}, Anka Bric^{1,*}, Julie Teruya-Feldstein², Andreas Herbst¹, Jonas A. Nilsson³, Carlos Cordon-Cardo², John L. Cleveland³, William P. Tansey¹, and Scott W. Lowe^{1,4}

¹Cold Spring Harbor Laboratory, 1 Bungtown Road, Cold Spring Harbor, New York 11724, USA

²Department of Pathology, Memorial Sloan Kettering Cancer Center, New York, New York 10021, USA

³Department of Biochemistry, St Jude Children's Research Hospital, Memphis, Tennessee 38105, USA

⁴Howard Hughes Medical Institute, Cold Spring Harbor, New York 11724, USA

Abstract

The *c-Myc* oncoprotein promotes proliferation and apoptosis, such that mutations that disable apoptotic programmes often cooperate with *MYC* during tumorigenesis. Here we report that two common mutant *MYC* alleles derived from human Burkitt's lymphoma uncouple proliferation from apoptosis and, as a result, are more effective than wild-type *MYC* at promoting B cell lymphomagenesis in mice. Mutant *MYC* proteins retain their ability to stimulate proliferation and activate p53, but are defective at promoting apoptosis due to a failure to induce the BH3-only protein Bim (a member of the B cell lymphoma 2 (Bcl2) family) and effectively inhibit Bcl2. Disruption of apoptosis through enforced expression of Bcl2, or loss of either *Bim* or *p53* function, enables wild-type *MYC* to produce lymphomas as efficiently as mutant *MYC*. These data show how parallel apoptotic pathways act together to suppress *MYC*-induced transformation, and how mutant *MYC* proteins, by selectively disabling a p53-independent pathway, enable tumour cells to evade p53 action during lymphomagenesis.

Human tumours frequently show deregulated expression of the *c-Myc* proto-oncogene^{1–3}. In Burkitt's lymphoma, this deregulation occurs through reciprocal translocations that juxtapose *c-Myc* with an immunoglobulin (Ig) promoter, leading to gross overexpression of *c-Myc* messenger RNA in the B cell lineage^{4,5}. In addition, point mutations are often found in the translocated *MYC* alleles, clustering in a conserved region known as MYC box I (refs 6–8). Although some mutations can increase *MYC* stability and transforming activity *in vitro*, their impact on the pathogenesis of Burkitt's lymphoma is unclear^{9–16}. In fact,

Reprints and permissions information is available at npg.nature.com/reprintsandpermissions.

Correspondence and requests for materials should be addressed to S.W.L. (lowe@cshl.org).

*These authors contributed equally to this work.

Supplementary Information is linked to the online version of the paper at www.nature.com/nature.

The authors declare no competing financial interests.

translocated *c-Myc* genes are subject to hypermutation *in vivo* that can also alter non-coding sequences, raising the possibility that these mutations are a consequence and not a cause of tumour development^{17,18}.

To examine the effects of *MYC* mutation on lymphoma development *in vivo*, we used a system for rapidly generating tissue-specific transgenic mice (see Supplementary Fig. 1). Two mutant *MYC* alleles commonly observed in Burkitt's lymphoma (P57S and T58A)¹³ were cloned into a murine stem cell virus (MSCV)-based vector that co-expresses green fluorescent protein (GFP). Haematopoietic stem cells (HSCs) derived from normal fetal livers were transduced with retroviruses expressing either wild-type or mutant *MYC*, and the genetically modified stem cells were then used to reconstitute the haematopoietic system of lethally irradiated recipient animals. This adoptive transfer strategy has several advantages over traditional transgenic approaches, such as: (1) transgene expression is limited to the haematopoietic system; (2) various combinations of transgenes or stem cell genotypes can be rapidly analysed; and (3) only a fraction of the injected stem cells are infected, allowing tumorigenesis to occur in the context of an essentially normal haematopoietic compartment. Also, the strong MSCV promoter produces high levels of *MYC* expression that recapitulate that observed in Burkitt's lymphoma (data not shown), and the co-expressed GFP enables assessment of infection efficiency and visualization of tumorigenesis using fluorescence imaging.

MYC* mutants show enhanced oncogenicity *in vivo

Although the control MSCV vector was not oncogenic (data not shown), recipients of stem cells infected with wild-type *MYC* developed tumours at low penetrance after a long latency (Fig. 1a; 2 out of 13 recipient mice at >100 days). The tumours that arose were aggressive pre-B cell lymphomas (Fig. 1b, c; see also Supplementary Fig. 2a), similar to those produced by the tissue-specific overexpression of *MYC* in transgenic mice¹⁹. Recipients of stem cells infected with the tumour-derived *MYC* point mutants also developed pre-B cell lymphomas, but at a significantly higher penetrance (Fig. 1a; 9 out of 12 for P57S and 8 out of 11 for T58A; $P < 0.005$ for each mutant versus wild-type *MYC*) and a significantly reduced latency (56 ± 9 days for P57S and 66 ± 9 days for T58A). Flow cytometry for GFP fluorescence showed that the increased tumorigenicity of these mutants was not due to differences in stem cell infection efficiency or transgene expression (see Supplementary Fig. 2b).

As deregulated *MYC* expression coordinately induces proliferation and apoptosis²⁰, the increased oncogenicity of the mutant *MYC* proteins might reflect the altered activation of one or both of these processes. To investigate the proliferation of cells expressing wild-type and mutant *MYC*, we assessed BrdU incorporation in the bone marrow of pre-malignant mice after stem cell reconstitution. Although all *MYC* constructs induced an increase in proliferation relative to uninfected controls (data not shown), wild-type and mutant *MYC* showed indistinguishable BrdU incorporation profiles (Fig. 2a; $25 \pm 3\%$ for wild-type *MYC*, $24 \pm 6\%$ for P57S and $27 \pm 5\%$ for T58A BrdU-positive cells). To examine the impact of *MYC* expression on apoptosis, we compared the ability of wild-type and mutant *MYC* to induce tumours in the presence of a strong apoptotic block. Recipient mice were

reconstituted with stem cells co-infected with a retrovirus expressing *MYC* constructs and a retrovirus expressing the anti-apoptotic protein Bcl2. Notably, when co-expressed with *Bcl2*, wild-type and mutant *MYC* produced aggressive B cell lymphomas with indistinguishable latency (34 ± 2 days for wild-type *MYC*, 35 ± 2 days for T58A and 33 ± 2 days for P57S) and penetrance (Fig. 2b, c). In addition, propidium iodide staining for DNA content revealed no differences in cell cycle profiles between lymphomas expressing wild-type and mutant *MYC* (Fig. 2d). Thus, in the absence of apoptosis, wild-type and mutant *MYC* are equally oncogenic.

Mutant *MYC* induces p19^{ARF} and p53, but not Bim

Oncogene-induced apoptosis is often mediated by the induction of p19^{ARF} and subsequent stabilization of p53, which is thought to sense hyperproliferative signals and prevent aberrant proliferation²¹. To investigate the basis for the apoptotic defect of mutant *MYC*, we examined p19^{ARF} and p53 expression in murine embryonic fibroblasts (MEFs) and HSC populations infected with wild-type and mutant *MYC* retroviruses. Interestingly, both P57S and T58A induced p19^{ARF} and p53 as well as (or better than) wild-type *MYC* (Fig. 3a, c). This p53 was transcriptionally active, as cells expressing either wild-type or mutant *MYC* showed a similar increase in p53 phosphorylation and expression of the p53 transcriptional targets *Bax*, *Puma* and *Noxa* (Fig. 3c and data not shown). Furthermore, the apoptotic defect was unrelated to the established ability of *MYC* to repress Bcl2 and Bcl-XL²², because no consistent effect of *MYC* on Bcl2 expression was observed and both wild-type and mutant *MYC* were capable of repressing Bcl-XL. Although p21^{Cip1} levels were reduced in HSCs expressing wild-type *MYC*, they were substantially higher in cells expressing mutant *MYC*. However, this effect was not consistently seen in MEFs (Fig. 3c and data not shown), suggesting that the impact of p21^{Cip1} repression on *MYC*-induced apoptosis²³ might contribute to, but is not essential for, the mutant *MYC* phenotype.

The pro-apoptotic, BH3-only protein Bim has recently been shown to inhibit *MYC*-induced lymphomagenesis, and Bim expression is elevated in B cells overexpressing *MYC* (ref. 24). Accordingly, Bim was acutely induced in response to wild-type *MYC* in MEFs, FL5.12 cells and HSCs (Fig. 3b, c; see also Supplementary Fig. 3a). This effect was not dependent on *MYC* induction of p53 because Bim was induced in *p53*^{-/-} MEFs (data not shown). However, both tumour-derived *MYC* mutants were unable to induce Bim efficiently. Furthermore, mice reconstituted with *Bim*^{-/-} stem cells expressing wild-type *MYC* produced lymphomas at a latency and penetrance indistinguishable from those reconstituted with *Bim*^{-/-} stem cells expressing mutant *MYC* (Fig. 3d, e; 40 ± 5 days for wild-type *MYC*, 36 ± 6 days for T58A and 38 ± 6 days for P57S), implying that the failure of these mutant *MYC* alleles to induce Bim contributes to their increased oncogenicity. Thus, *MYC* mutations do not affect the 'sensing' of *MYC* induced hyperproliferative signals by the p19^{ARF}-p53 pathway, but promote lymphomagenesis by abrogating a parallel apoptotic signal transmitted from *MYC* to Bim.

Bim was initially identified by virtue of its ability to bind Bcl2, and it acts as a potent inhibitor of the pro-survival members of the Bcl2 family²⁵. Thus, failure of mutant *MYC* to induce Bim should result in a defective ability to suppress Bcl2 activity. Such a model

predicts that suppression of Bcl2 activity might rescue the apoptotic defect of mutant *MYC*. To test this, we assessed the ability of wild-type and mutant *MYC* to promote apoptosis in cells derived from *Bcl2* knockout mice. Wild-type (*Bcl2*^{+/+}) and *Bcl2*-deficient (*Bcl2*^{-/-}) MEFs were infected with retroviruses expressing each *MYC* allele and then subjected to serum starvation to trigger apoptosis. In the presence of *Bcl2*, wild-type *MYC* consistently induced higher levels of apoptosis than either of the *MYC* point mutants (Fig. 3f). However, in *Bcl2*^{-/-} MEFs, P57S and T58A were as capable of inducing apoptosis as wild-type *MYC*. Interestingly, apoptosis induced by wild-type *MYC* was not affected by *Bcl2* ablation, perhaps because wild-type *MYC* already efficiently inhibits Bcl2. Similarly, recipients of *Bcl2*^{+/+} HSCs infected with wild-type *MYC* showed significantly less GFP-positive bone marrow after reconstitution compared with those receiving mutant *MYC*-infected stem cells; however, all *MYC*-expressing cells were strongly selected against during haematopoietic reconstitution with *Bcl2*^{-/-} HSCs (see Supplementary Fig. 3b). Thus, in the absence of *Bcl2*, wild-type and mutant *MYC* were equally capable of promoting cell death, implying that *MYC* mutants—through reduced Bim induction and perhaps other additional effects—are ultimately deficient in their ability to inhibit Bcl2.

Evasion of p53 tumour suppressor function

These data suggest that the increased oncogenicity of tumour-derived *MYC* point mutants results from their inability to efficiently couple proliferation to cell death. Certain targeted apoptotic defects can obviate the requirement for tumour suppressor inactivation during tumorigenesis. For example, both *Bcl2* overexpression and *Bim* deficiency facilitate *MYC*-induced lymphomagenesis in the absence of *p19*^{ARF} or *p53* mutations^{24,26}. To determine whether *MYC* point mutations could also bypass the requirement for *p53* loss, we examined tumour onset and *p53* status in lymphomas derived from *p53*^{+/-} stem cells. In this context, both wild-type and mutant *MYC* rapidly produced lymphomas with complete penetrance (Fig. 4a), although those produced by wild-type *MYC* arose with slightly longer latency (56 ± 24 days for wild-type *MYC*, 35 ± 3 days for T58A and 40 ± 9 days for P57S; *P* < 0.001 for both mutants compared with wild type). However, although tumours induced by wild-type *MYC* invariably lost the wild-type *p53* allele during tumour development (0 out of 9 with wild-type *p53* allele), those induced by the *MYC* mutants typically retained the wild-type *p53* allele (7 out of 9 with wild-type *p53* allele for both P57S and T58A; Fig. 4a, inset).

The requirement to lose the wild-type *p53* allele in tumours initiated by wild-type *MYC* may account for their delayed onset relative to tumours in recipients of mutant *MYC*-infected stem cells. Indeed, mice reconstituted with *p53*^{-/-} HSCs expressing either the wild-type or mutant *MYC* formed tumours rapidly, with an identical penetrance and latency (Fig. 4b; 40 ± 8 days for wild-type *MYC*, 40 ± 4 days for T58A and 41 ± 5 days for P57S). All of the *p53*^{-/-} lymphomas were oligoclonal (see Supplementary Fig. 3b), and showed no obvious differences between wild-type and mutant *MYC* expression (Fig. 4b, inset). Thus *MYC* mutations can facilitate tumour development in the absence of *p53* inactivation.

MYC, p53 and Bim status in Burkitt's lymphoma

These data predict that Bim expression should be reduced in Burkitt's lymphomas expressing *MYC* mutations, and that *p53* mutations should be under-represented in Burkitt's lymphomas harbouring the P57S and T58A mutant *MYC* alleles. Indeed, seven out of seven Burkitt's lymphomas expressing wild-type *MYC* were positive for Bim expression by immunohistochemistry, displaying substantially higher Bim levels than several diffuse, large B cell lymphomas (DLBCL) without *MYC* translocations (three out of three; Fig. 4c). In contrast, six out of seven Burkitt's lymphomas harbouring *MYC* alleles with *MYC* box I mutations (including four out of five tumours with P57 and T58 mutations) were scored as Bim negative (Fig. 4c). Furthermore, none of the *p53* mutant Burkitt's lymphomas (0 out of 17) that we analysed or identified from the literature^{6,27,28} had coincident mutations at *MYC* codons 57 and 58, despite their common occurrence in our data set (12 out of 71) (see Supplementary Table; and data not shown). Of note, two out of two lymphomas harbouring a Pro to Ser mutation at codon 60 of *MYC* had a *p53* mutation at codon 248, suggesting that not all *MYC* mutations are equivalent. Nevertheless, our data demonstrate that two mutant *MYC* alleles commonly observed in Burkitt's lymphoma can bypass p53 action during lymphomagenesis in mice, and provide evidence to suggest that this may also occur in humans.

Discussion

Our results reveal new insights into the biology of the *MYC* oncoprotein. For example, they suggest that tumour-derived *MYC* mutants are relevant to the pathology of Burkitt's lymphoma because they are unable to upregulate Bim and efficiently inhibit Bcl2. Furthermore, they show that the *MYC* mutants we examined retain their ability to activate the p19^{ARF}-p53 pathway and efficiently promote proliferation. Thus, *MYC* mutations alter *MYC* activity in both quantitative^{12,14} and, as shown here, qualitative ways. These qualitative changes may be particularly important for the development of tumours such as Burkitt's lymphoma, which acquire independent alterations that quantitatively upregulate *MYC*. Such qualitative changes to *MYC* may also be important for normal cell growth; in this regard, some tumour-derived *MYC* mutations lead to constitutive phosphorylation of *MYC* at Ser 62, a target of mitogen-stimulated kinases¹⁴. Perhaps *MYC* mutations 'lock in' a qualitative state that normally uncouples proliferation from apoptosis in response to mitogens, allowing tissue expansion.

Mutations that are selected for in malignant tumours pinpoint genes and processes that must be altered during tumour evolution. Thus, the fact that certain mutant *MYC* alleles selected for in human lymphomas are specifically impaired in their ability to promote apoptosis *in vivo* provides compelling genetic evidence that the phenomenon of oncogene-induced apoptosis is relevant to human tumorigenesis. Furthermore, our results demonstrate that the *MYC*-induced apoptotic programme is not linear, but instead involves p53-dependent and -independent signals that act in parallel to promote cell death and suppress *MYC*-induced tumorigenesis. That a cell expressing mutant *MYC* can activate p53 in response to hyperproliferative signalling but evade p53 action implies that *MYC*-induced apoptosis involves a threshold phenomenon, such that inactivation of any one of several *MYC*

effectors can cause apoptotic firing to drop below the threshold level and allow unabated proliferation. Consequently, certain mutations in *MYC* alleviate the requirement for a cooperating gene mutation during tumorigenesis.

METHODS

Retroviral infection and cell culture

HAM (a methionine-rich variant of the widely used haemagglutinin tag)-tagged wild-type *MYC* and mutants were subcloned into MSCV-IRES-GFP²⁶ for *in vivo* studies and MSCVpuro (Clon-tech) for cell culture studies. Primary MEFs were generated from embryonic 13.5 (E13.5) day embryos from a wild-type C57BL/6J background or from a *Bcl2*^{+/-} to *Bcl2*^{+/-} cross. Retroviral-mediated gene transfer was performed using Phoenix packaging cells as previously described²⁹. Cells for *in vivo* studies were infected with MSCV-GFP, MSCV-GFP-WT *MYC*, MSCV-GFP-P57S or MSCV-GFP-T58A. Infected cell populations of FL5.12 cells and MEFs used for *in vitro* studies were selected in puromycin (2 mg ml⁻¹ for 2 days). Infected HSCs used for *in vitro* studies were diluted to equal infection efficiency (assessed by GFP) then sorted using magnetic beads to 70–80% purity with a lineage cell depletion kit (Miltenyi Biotec). For cell viability assays, MEFs were infected with *MYC*-expressing retroviruses as described, and were incubated for 24 h in either 10% fetal bovine serum (high serum) or 0.1% fetal bovine serum (low serum) and analysed for viability by trypan blue exclusion.

Stem cell isolation and adoptive transfer

Pregnant E14.5 C57BL/6 mice from wild-type, *p53*^{+/-}, *Bim*^{+/-} or *Bcl2*^{+/-} crosses were killed to obtain fetal livers. Stem cell infection and transplantation were performed as described²⁶. For stem cell reconstitution and BrdU analysis, total bone marrow was isolated 21–28 days after tail vein injection. *In vivo* BrdU incorporation was assessed using an APC BrdU Flow Kit (BD Pharmingen). Bone marrow was harvested 2 h after an intraperitoneal injection of 200 ml 10 mg ml⁻¹ BrdU, and BrdU incorporation was assessed for a population of GFP-positive cells at a defined GFP intensity. Flow cytometry analysis was performed on a Becton Dickinson LSRII cell analyser, with FACSVantage DiVa software.

Lymphoma monitoring and analysis

Reconstituted animals were monitored for illness by lymph node palpation, monitoring overall morbidity, and, in some cases, whole-body fluorescence imaging²⁶. Overall survival was defined as the time from stem cell reconstitution until the animal reached a terminal stage and was killed. Statistical analysis was performed using a one-way ANOVA (analysis of variance) test using Graph Pad Prism version 3.0 (Graph Pad Software). Immunohistochemistry was performed using CD45R/B220-clone RA3-6B2 (BD Biosciences, Pharmingen) and rabbit anti-Bim (Stressgen) antibodies. Tumour cell DNA content was determined by FACS analysis with propidium iodide staining of ethanol-fixed cells²⁶. Nested PCR analysis of variable, diversity and joining (V(D)J) recombination was performed as described³⁰.

Protein analysis

Immunoblots were performed from whole-cell lysates obtained by boiling cell pellets that were solubilized in Laemmli sample buffer. Twenty micrograms of protein samples (Bio-Rad protein assay) were separated by SDS polyacrylamide electrophoresis (SDS-PAGE) and transferred to Immobilon-P membranes (Millipore). The antibodies used were anti-MYC (Ab1, Oncogene; 1:250), anti-p19^{ARF} (ab80-100, Abcam; 1:1,000), anti-p21 (C-19, Santa Cruz; 1:500), anti-p53 (NCL-p53-505, Novocastra; 1:500), anti-phosphop53 (Ser 15) (16G8, Cell Signaling; 1:1,000), anti-Bim/BOD (AAP-330, Stressgen; 1:1,000), anti-Bcl2 (N-19, Santa Cruz; 1:1,000) and anti-Bcl-XL (S-18, Santa Cruz; 1:1,000). Proteins were visualized using ECL (Amersham) or Lumi-light (Roche).

Supplementary Material

Refer to Web version on PubMed Central for supplementary material.

Acknowledgements

We thank M. S. Jiao, C. Rosenthal, M. Yang, S. Ray, C. Yang and I. Linkov for technical assistance and J. Zilfou, R. Dickins, E. Cepero, M. Spector, J. Fridman and other members of the Lowe laboratory for advice and/or critical reading of the manuscript. We also thank A. Hunt and G. Evan for helpful advice, and T. Mak and A. Strasser for mice. This work was supported by a postdoctoral fellowship from the Helen Hay Whitney Foundation (M.T.H.), an NCI postdoctoral training grant (A.B.), a program project grant from the National Cancer Institute (W.P.T and S.W.L.) and a grant from the Irving Hansen Memorial Foundation (W.P.T). W.P.T. is a Leukemia and Lymphoma Society Scholar and S.W.L. is an AACR-NCRF Research Professor.

References

1. Dang CV. c-Myc target genes involved in cell growth, apoptosis, and metabolism. *Mol. Cell. Biol.* 1999; 19:1–11. [PubMed: 9858526]
2. Cole MD. Activation of the c-myc oncogene. *Basic Life Sci.* 1986; 38:399–406. [PubMed: 3741337]
3. Spencer CA, Groudine M. Control of c-myc regulation in normal and neoplastic cells. *Adv. Cancer Res.* 1991; 56:1–48. [PubMed: 2028839]
4. Dalla-Favera R, et al. Human c-myc onc gene is located on the region of chromosome 8 that is translocated in Burkitt lymphoma cells. *Proc. Natl Acad. Sci. USA.* 1982; 79:7824–7827. [PubMed: 6961453]
5. Davis M, Malcolm S, Rabbitts TH. Chromosome translocation can occur on either side of the c-myc oncogene in Burkitt lymphoma cells. *Nature.* 1984; 308:286–288. [PubMed: 6700731]
6. Bhatia K, et al. Point mutations in the c-Myc transactivation domain are common in Burkitt's lymphoma and mouse plasmacytomas. *Nature Genet.* 1993; 5:56–61. [PubMed: 8220424]
7. Albert T, Urlbauer B, Kohlhuber F, Hammersen B, Eick D. Ongoing mutations in the N-terminal domain of c-Myc affect transactivation in Burkitt's lymphoma cell lines. *Oncogene.* 1994; 9:759–763. [PubMed: 8108117]
8. Clark HM, et al. Mutations in the coding region of c-MYC in AIDS-associated and other aggressive lymphomas. *Cancer Res.* 1994; 54:3383–3386. [PubMed: 8012955]
9. Henriksson M, Bakardjiev A, Klein G, Luscher B. Phosphorylation sites mapping in the N-terminal domain of c-myc modulate its transforming potential. *Oncogene.* 1993; 8:3199–3209. [PubMed: 8247524]
10. Hoang AT, et al. A link between increased transforming activity of lymphoma-derived MYC mutant alleles, their defective regulation by p107, and altered phosphorylation of the c-Myc transactivation domain. *Mol. Cell. Biol.* 1995; 15:4031–4042. [PubMed: 7623799]

11. Westaway D, Payne G, Varmus HE. Proviral deletions and oncogene base-substitutions in insertionally mutagenized c-myc alleles may contribute to the progression of avian bursal tumors. *Proc. Natl Acad. Sci. USA.* 1984; 81:843–847. [PubMed: 6322173]
12. Salghetti SE, Kim SY, Tansey WP. Destruction of Myc by ubiquitin-mediated proteolysis: cancer-associated and transforming mutations stabilize Myc. *EMBO J.* 1999; 18:717–726. [PubMed: 9927431]
13. Chang DW, Claassen GF, Hann SR, Cole MD. The c-Myc transactivation domain is a direct modulator of apoptotic versus proliferative signals. *Mol. Cell. Biol.* 2000; 20:4309–4319. [PubMed: 10825194]
14. Sears RC. The life cycle of c-Myc: from synthesis to degradation. *Cell Cycle.* 2004; 3:1133–1137. [PubMed: 15467447]
15. Frykberg L, Graf T, Vennstrom B. The transforming activity of the chicken c-myc gene can be potentiated by mutations. *Oncogene.* 1987; 1:415–422. [PubMed: 3330784]
16. Yeh E, et al. A signalling pathway controlling c-Myc degradation that impacts oncogenic transformation of human cells. *Nature Cell Biol.* 2004; 6:308–318. [PubMed: 15048125]
17. Rabbitts TH, Hamlyn PH, Baer R. Altered nucleotide sequences of a translocated c-myc gene in Burkitt lymphoma. *Nature.* 1983; 306:760–765. [PubMed: 6419122]
18. Bemark M, Neuberger MS. The c-MYC allele that is translocated into the IgH locus undergoes constitutive hypermutation in a Burkitt's lymphoma line. *Oncogene.* 2000; 19:3404–3410. [PubMed: 10918597]
19. Adams JM, et al. The c-myc oncogene driven by immunoglobulin enhancers induces lymphoid malignancy in transgenic mice. *Nature.* 1985; 318:533–538. [PubMed: 3906410]
20. Evan GI, et al. Induction of apoptosis in fibroblasts by c-myc protein. *Cell.* 1992; 69:119–128. [PubMed: 1555236]
21. Lowe SW, Sherr CJ. Tumor suppression by Ink4a-Arf: progress and puzzles. *Curr. Opin. Genet. Dev.* 2003; 13:77–83. [PubMed: 12573439]
22. Maclean KH, Keller UB, Rodriguez-Galindo C, Nilsson JA, Cleveland JL. c-Myc augments gamma irradiation-induced apoptosis by suppressing Bcl-XL. *Mol. Cell. Biol.* 2003; 23:7256–7270. [PubMed: 14517295]
23. Seoane J, Le HV, Massague J. Myc suppression of the p21(Cip1) Cdk inhibitor influences the outcome of the p53 response to DNA damage. *Nature.* 2002; 419:729–734. [PubMed: 12384701]
24. Egle A, Harris AW, Bouillet P, Cory S. Bim is a suppressor of Myc-induced mouse B cell leukemia. *Proc. Natl Acad. Sci. USA.* 2004; 101:6164–6169. [PubMed: 15079075]
25. O'Connor L, et al. Bim: a novel member of the Bcl-2 family that promotes apoptosis. *EMBO J.* 1998; 17:384–395. [PubMed: 9430630]
26. Schmitt CA, et al. Dissecting p53 tumour suppressor functions *in vivo*. *Cancer Cell.* 2002; 1:289–298. [PubMed: 12086865]
27. Gaidano G, et al. p53 mutations in human lymphoid malignancies: association with Burkitt lymphoma and chronic lymphocytic leukemia. *Proc. Natl Acad. Sci. USA.* 1991; 88:5413–5417. [PubMed: 2052620]
28. Bhatia KG, Gutierrez MI, Huppi K, Siwarski D, Magrath IT. The pattern of p53 mutations in Burkitt's lymphoma differs from that of solid tumors. *Cancer Res.* 1992; 52:4273–4276. [PubMed: 1638540]
29. Serrano M, Lin AW, McCurrach ME, Beach D, Lowe SW. Oncogenic ras provokes premature cell senescence associated with accumulation of p53 and p16INK4a. *Cell.* 1997; 88:593–602. [PubMed: 9054499]
30. Yu D, Thomas-Tikhonenko A. A non-transgenic mouse model for B-cell lymphoma: *in vivo* infection of p53-null bone marrow progenitors by a Myc retrovirus is sufficient for tumorigenesis. *Oncogene.* 2002; 21:1922–1927. [PubMed: 11896625]

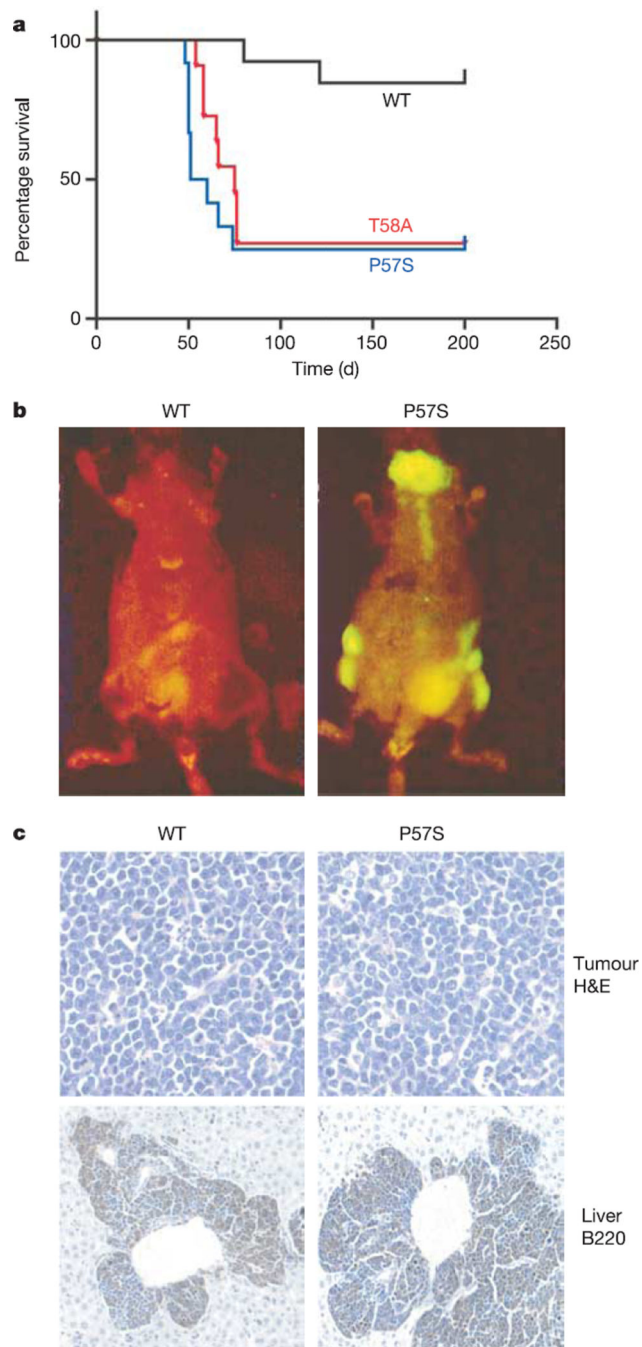


Figure 1. Tumour-derived *MYC* mutants show enhanced oncogenicity *in vivo*

a, Kaplan–Meier curve showing survival at various times after adoptive transfer. **b**, *In vivo* GFP imaging shows disseminated lymphomas in a mouse 60 days after reconstitution with HSCs transduced with P57S, but not wild-type *MYC*. **c**, Haematoxylin/eosin staining and immunohistochemical staining for B220 (a B cell lineage marker) of lymph node and liver sections of animals harbouring wild-type *MYC* and P57S lymphomas, showing an aggressive B cell disease with perivascular infiltration of B220-positive tumour cells into the liver.

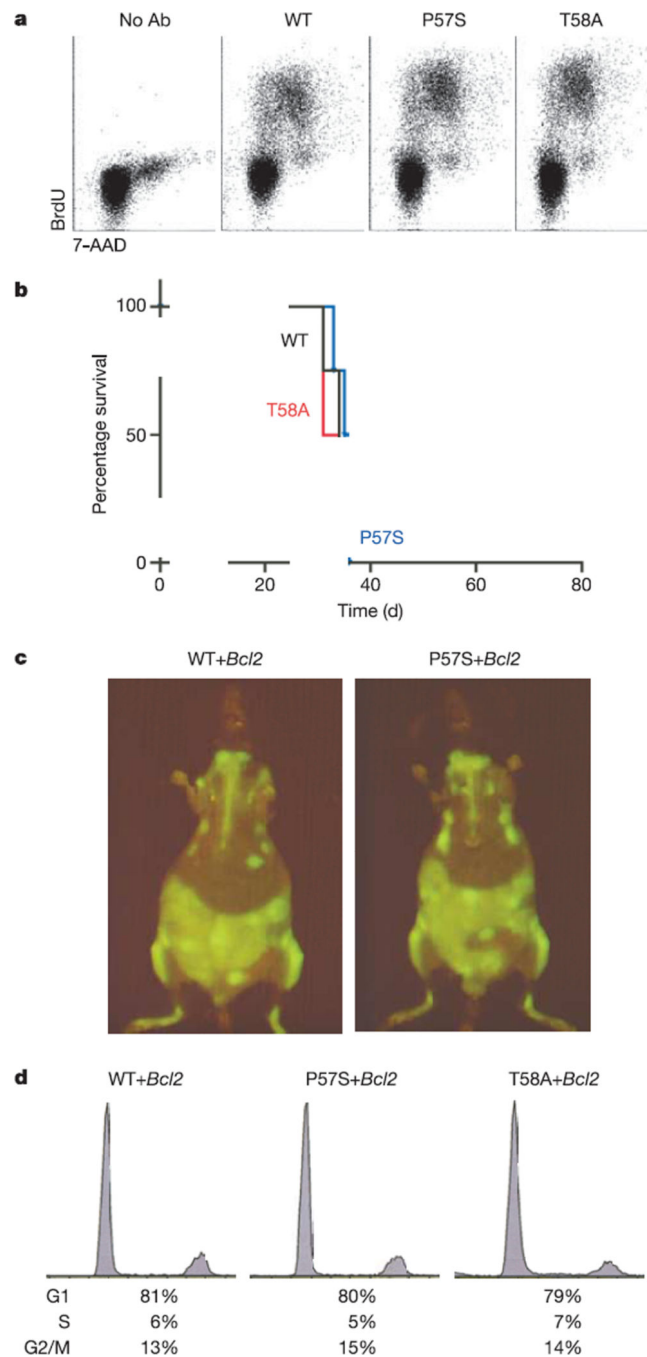


Figure 2. Wild-type and mutant MYC show apoptotic, but not proliferative, differences *in vivo*
a, Flow cytometry showing BrdU incorporation in GFP-positive bone marrow cells 24 days after reconstitution. Data are representative of three independent experiments. **b**, Kaplan–Meier curve showing survival following adoptive transfer with HSCs co-infected with the indicated MYC-expressing retroviruses and a Bcl2-expressing retrovirus. **c**, *In vivo* GFP imaging showing disseminated lymphomas in mice 35 days after adoptive transfer with HSCs co-transduced with wild-type or mutant MYC and Bcl2. **d**, Representative histograms of DNA content of wild-type MYC/Bcl2 and mutant MYC/Bcl2 lymphomas.

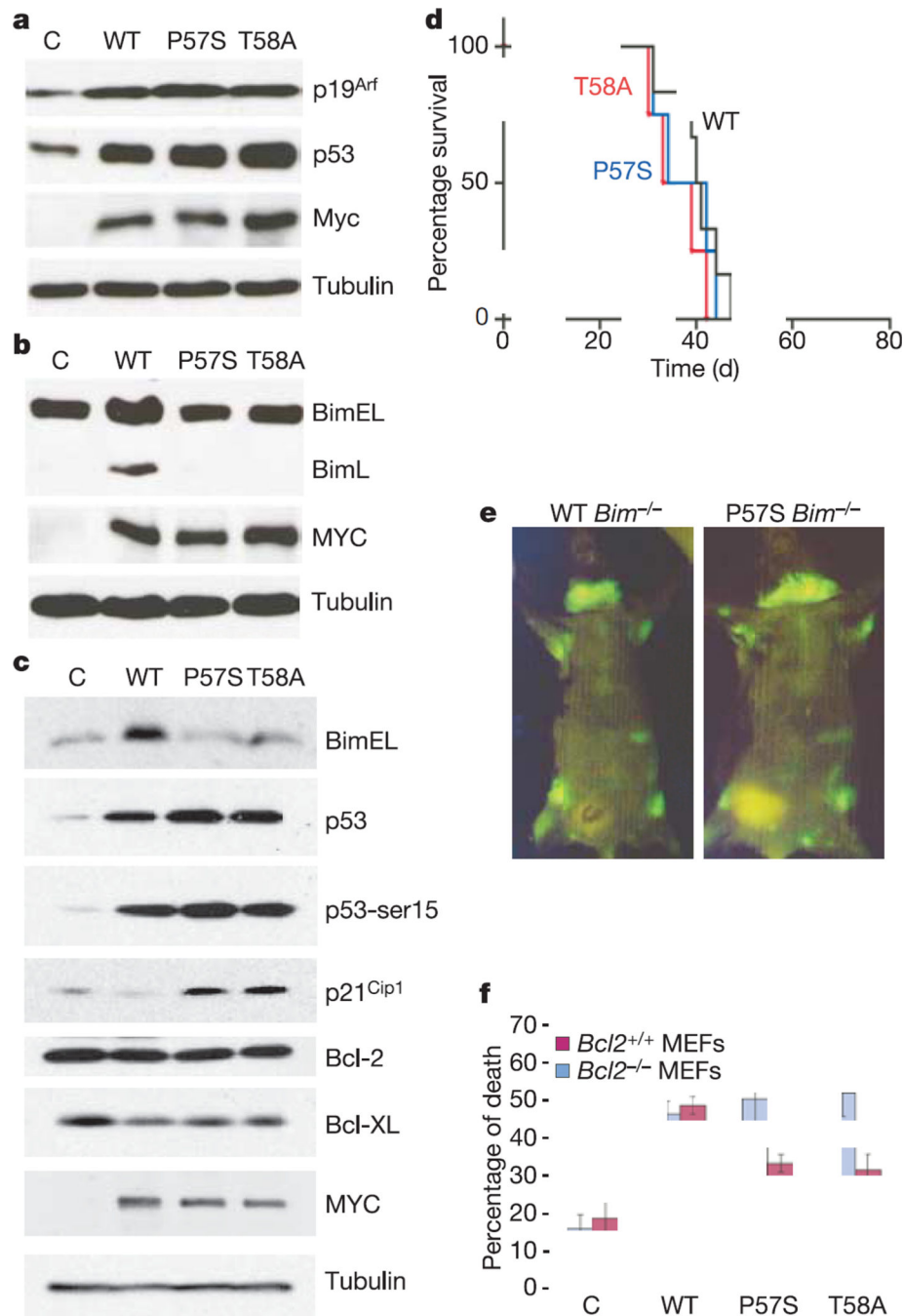


Figure 3. Impaired Bim induction contributes to the increased oncogenicity of mutant *MYC* alleles

a, b, Western blot analysis showing ARF and p53 levels (**a**) or Bim levels (**b**) in MEFs stably infected with control (labelled C), wild-type *MYC* or mutant *MYC* vectors. The long (BimL) and extra long (BimEL) isoforms of Bim are shown. **c**, Western blot analysis of HSCs using antibodies against the indicated proteins. **d**, Kaplan–Meier curve showing free–free survival following adoptive transfer with *Bim*^{-/-} HSCs infected with the indicated *MYC*-expressing retroviruses. **e**, *In vivo* GFP imaging showing disseminated lymphomas in

mice 34 days after adoptive transfer with *Bim*^{-/-} HSCs transduced with mutant or wild-type *MYC*. f, Wild type (*Bcl2*^{+/+}) and *Bcl2*^{-/-} MEFs transduced with the indicated retroviruses were incubated in low serum and viability was assessed by trypan blue exclusion. Data represent the mean ± standard deviation of three independent experiments.

Author Manuscript

Author Manuscript

Author Manuscript

Author Manuscript

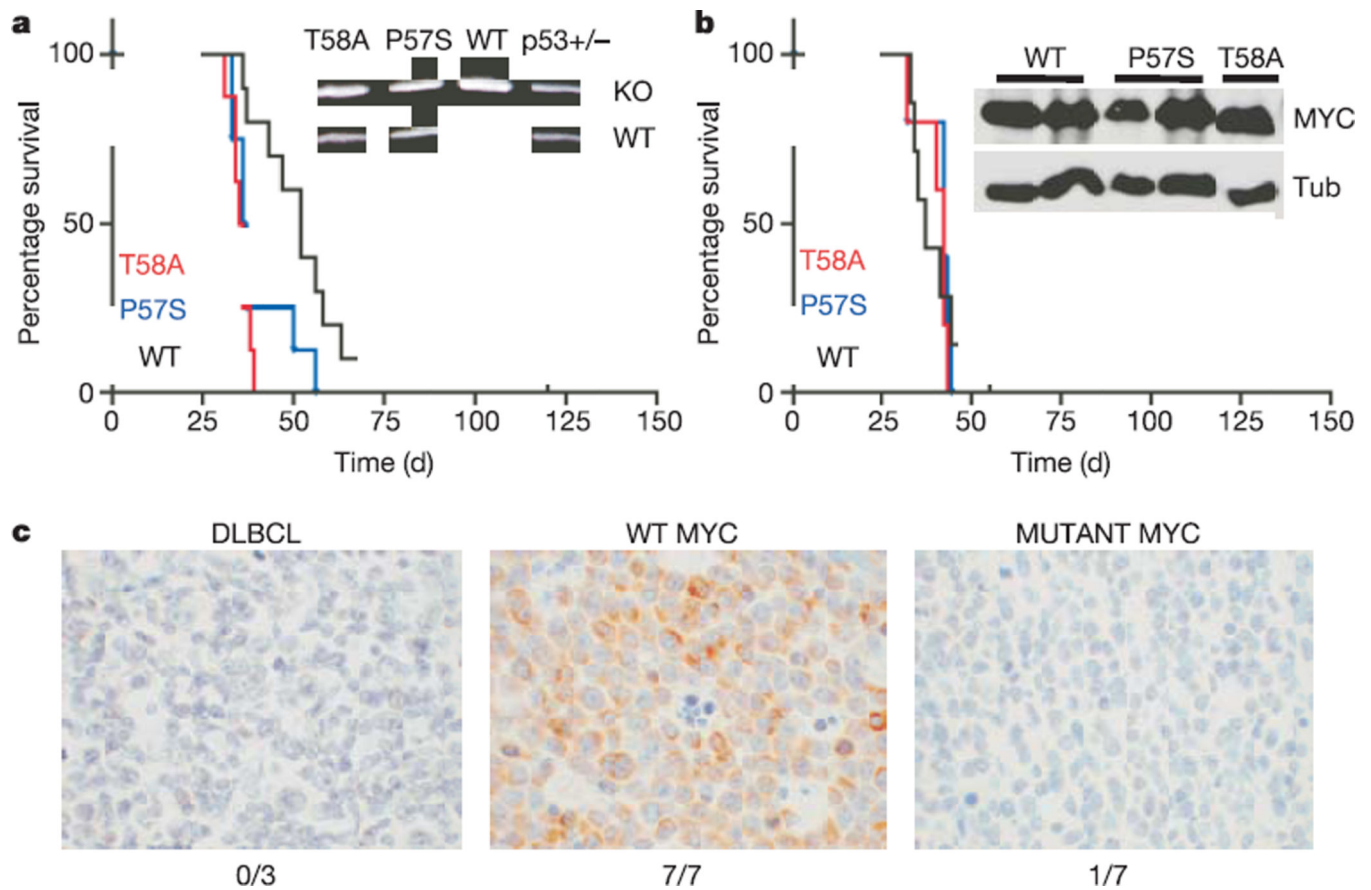


Figure 4. Impact of mutations in *MYC* on *p53* tumour suppressor action and Bim induction in human Burkitt's lymphomas

a, Kaplan–Meier curve showing mouse survival after adoptive transfer with *p53*^{+/-} HSCs infected with the indicated *MYC* retroviral constructs. Inset, Representative allele-specific PCR assay showing retention of the wild-type *p53* allele in lymphomas produced by mutant but not wild-type *MYC*. **b**, Kaplan–Meier curve showing mouse survival after adoptive transfer with *p53*^{-/-} HSCs infected as in **a**. Inset, western blot analysis of representative lymphomas harbouring the indicated *MYC* allele. **c**, Bim expression in DLBCL and wild-type *MYC*-expressing and mutant *MYC*-expressing Burkitt's lymphomas as assessed by immunohistochemistry using an anti-Bim antibody. The frequency of Bim-positive tumours in each category is indicated.